Journal of Ceramic Processing Research. Vol. 17, No. 6, pp. 591~595 (2016)

J O U R N A L O F
Ceramic Processing Research

Enhanced facture toughness of (W,Ti)C by addition of CNT

In-Jin Shon*

Division of Advanced Materials Engineering, the Research Center of Hydrogen Fuel Cell, Chonbuk National University, 664-14 Deokjin-dong 1-ga, Deokjin-gu, Jeonju, Jeonbuk 561-756, Korea

The grain size of (W,Ti)C powder remarkably decreases with a high-energy ball milling. The rapid sintering of nanostructured (W,Ti)C and (W,Ti)C-5 vol.%CNT hard materials was investigated with high frequency induction heating. The advantage of this process is that it allows very quick densification to near theoretical density and prohibition of grain growth in nanostructured materials. A dense nanostructured (W,Ti)C and (W,Ti)C-5 vol.%CNT hard material with a relative density of up to 99% was produced with simultaneous application of 80 MPa pressure and induced output current with total power capacity of 15 kW within 3 minutes. The effect of CNT on the sintering behavior and mechanical properties of (W,Ti)C was investigated. The fracture toughness of (W,Ti)C increased by addition of CNT.

Key words: Nanomaterials, Sintering, Hardness, Fracture toughness, Powder metallurgy.

Introduction

(W,Ti)C has a high melting point and high hardness. In this regard, the transition metal carbide is primarily used as cutting tools and abrasive materials as a single phase or composite structures. In the case of cemented (W,Ti)C, Co or Ni is added as a binder for the formation of composite structures. However, the high cost of Co or Ni and the low corrosion resistance of the (W,Ti)C-Co or (W,Ti)C-Ni cermet have generated interest in recent years to find alternative binder phases [1-4]. It has been reported that CNT shows a high hardness, elastic modulus, strength, good resistance to corrosion and cheaper material when compared to Co and Ni [5].

Nanocrystalline materials have received much attention as advanced engineering materials with excellent physical and mechanical properties [6, 7]. Recently, nanocrystalline powders have been developed using a thermochemical, thermomechanical spray conversion process (SCP), co-precipitation and high energy milling [8-10]. Among the methods, the sintering temperature of the high energy mechanical milled powder is lower than that of the unmilled powder, due to the increase in the reactivity of the powder, the internal and surface energy as well as the surface area, which all contribute to its so-called mechanical activation. However, the grain size in sintered materials becomes much larger than that in pre-sintered powders due to fast grain growth during conventional sintering. Therefore, even though the initial particle size is less than 100 nm, the grain size increases rapidly up to 2 μm or larger during conventional sintering [11]. Controlling grain growth during sintering is one of the keys to the commercial success of nanostructured materials. In this regard, the high frequency induction heated sintering method (HFIHS), which can make dense materials within 2 minutes, has been shown to be effective in achieving this goal [12-15].

In this study, we investigated the effect of CNT on sintering behavior and mechanical properties of the (W,Ti)C by the HFIHS method. The goal of this research is to produce nanopowder and dense nanostructured (W,Ti)C and (W,Ti)C-5 vol.%CNT composites.

Experimental Procedures

The (W,Ti)C powder with a grain size of < 1 mm and 99% purity and CNT used in this research was supplied by H.C. Starck and Carbon nanotechnology Inc. respectively. The powders were first milled in a high-energy ball mill (Pulverisette-5 planetary mill) at 250 rpm for 10 h. Tungsten carbide balls (9 mm in diameter) were used in a sealed cylindrical stainless steel vial under an argon atmosphere. The weight ratio of balls-to-powder was 30 : 1. Milling resulted in a significant reduction in grain size. The grain size of the (W,Ti)C was calculated from the full width at half-maximum (FWHM) of the diffraction peak by Suryanarayana and Grant Norton's formula [16].

$$B_r(B_{crystalline} + B_{strain})\cos\theta = k\,\lambda/L + \eta\sin\theta \quad (1)$$

where B_r is the full width at half-maximum (FWHM) of the diffraction peak after instrumental correction; $B_{crystalline}$ and B_{strain} are the FWHM caused by the small

*Corresponding author:
Tel : +82-63-270-2381
Fax: +82-63-270-2386
E-mail: ijshon@chonbuk.ac.kr

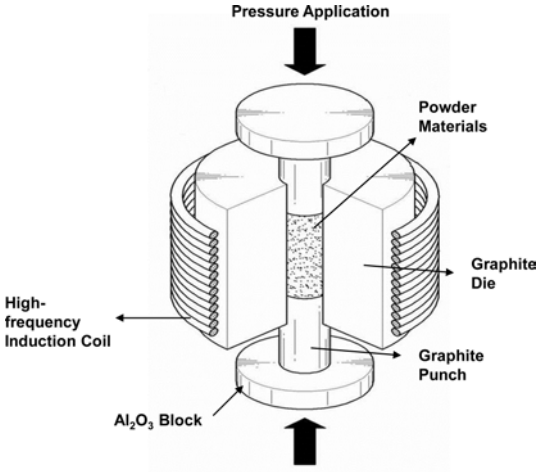

Fig. 1. Schematic diagram of the apparatus for high-frequency induction heated sintering.

grain size and internal stress, respectively; k is a constant (with a value of 0.9); λ is the wavelength of the X-ray radiation; L and η are the grain size and internal strain, respectively; and θ is the Bragg angle. The parameters B and B_r follow Cauchy's form with the relationship: $B = B_r + B_s$, where B and B_s are the FWHM of the broadened Bragg peaks and the standard sample's Bragg peaks, respectively.

The powders were placed in a graphite die (outside diameter, 45 mm; inside diameter, 20 mm; height, 40 mm) and then introduced into the high-frequency induction heating sintering (HFIHS) apparatus shown schematically in Fig. 1. The HFIHS apparatus includes a 15 kW power supply that provides an induced current through the sample, and 50 kN uniaxial press. The system was first evacuated and a uniaxial pressure of 80 MPa was applied. An induced current was then activated and maintained until the densification rate was negligible, as indicated by real-time output of the shrinkage of the sample. The shrinkage was measured by a linear gauge measuring the vertical displacement. The HFIHS can be controlled in two ways: by temperature control or by output control. The latter was chosen to investigate the effect of the output of total power, given that the induced current level has a direct effect on the rate of heating and on the maximum temperature. The output level was 80% of the output of total power. Temperatures were measured by a pyrometer focused on the surface of the graphite die. At the end of the process, the induced current was turned off and the sample cooled to room temperature. The process was carried out under a vacuum of 5.33 Pa.

The relative density of the sintered sample was measured by the Archimedes method. Microstructural information was obtained from product samples which had been polished and etched using Murakami's reagent (10 g potassium ferricyanide, 10 g NaOH, and 100 mL water) for 1-2 min at room temperature. Compositional and microstructural analyses of the products were made through X-ray diffraction (XRD), scanning electron microscopy (SEM) with energy dispersive spectroscopy (EDS) and field emission scanning electron microscope (FE-SEM). Vickers hardness was measured by indentations at a load of 10 kg_f and a dwell time of 15 s.

Results and Discussion

Fig. 2 shows FE-SEM images of the (W,Ti)C, and (W,Ti)C-5 vol.%CNT powders after milling for 10h. (W,Ti)C powder has a nano-size, round shape and some agglomeration. EDS of (W,Ti)C-5vol.%CNT powder milled for 10 h is shown in Fig. 3. In EDS W, Ti and C peaks are detected. The milling process is known to introduce impurities from the ball and/or container. However, in this study, peaks of Fe was not identified.

The variations of the shrinkage displacement and temperature with the heating time for an induced current during the sintering of the high energy ball milled (W,Ti)C and (W,Ti)C-5 vol.%CNT powders under a pressure of 80 MPa are shown in Fig. 4. In all cases, the application of the induced current resulted in shrinkage due to consolidation. The shrinkage of (W,Ti)C and (W,Ti)C-5 vol.%CNT powders is nearly constant up to 900 °C. And then the shrinkage of two powder rapidly increased above the temperature.

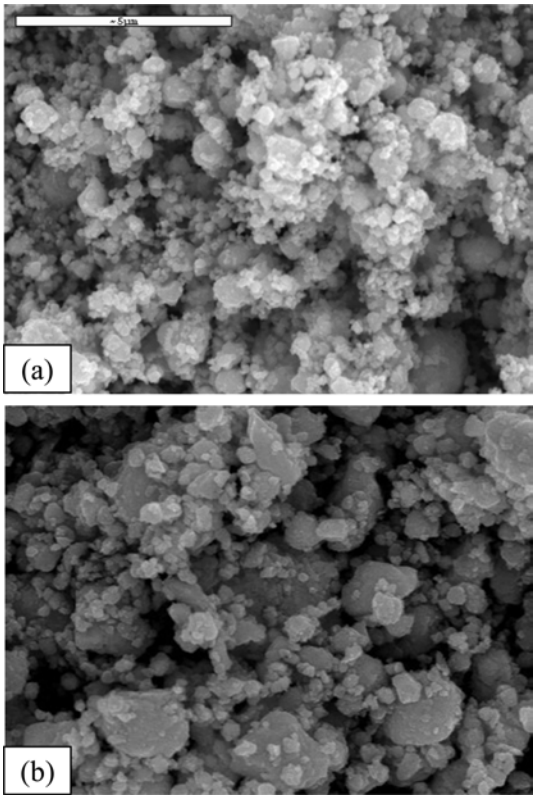

Fig. 2. FE-SEM images of (a) (W,Ti)C and (b) (W,Ti)C-5 vol.%CNT powders after milling for 10 h.

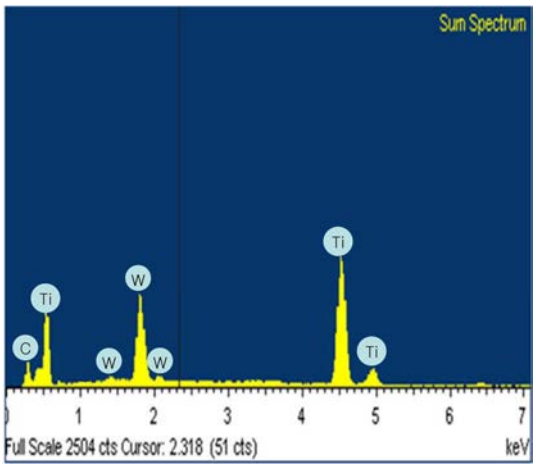

Fig. 3. EDS of the (W,Ti)C-5 vol.%CNT powders with milling for 10 h.

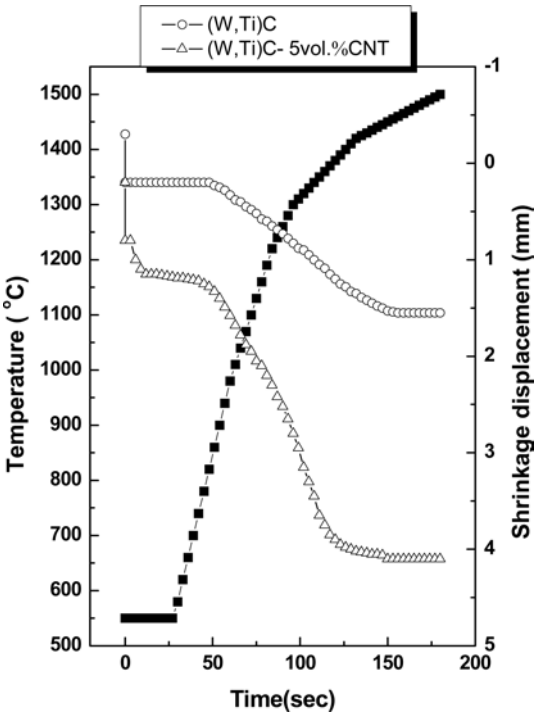

Fig. 4. Variations of temperature and shrinkage with heating time during the pulsed current activated sintering of (W,Ti)C and (W,Ti)C-5 vol.%CNT powders milled for 10 h.

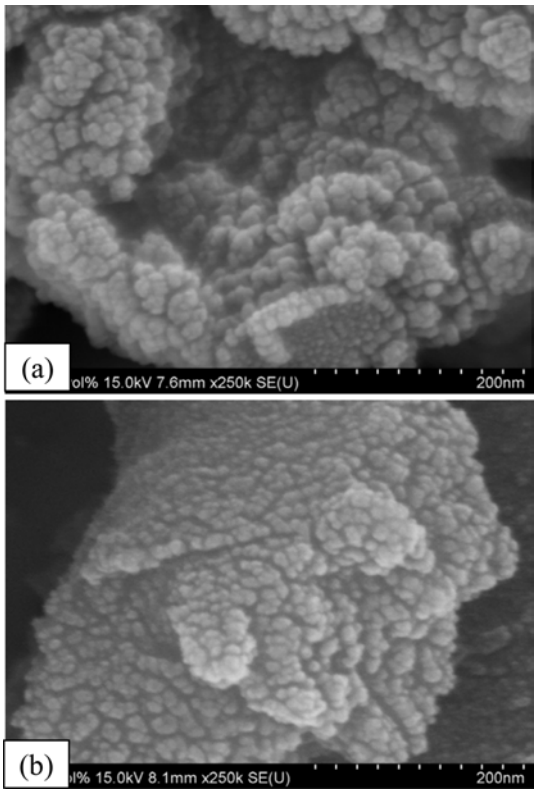

Fig. 5. FE-SEM images of (a) (W,Ti)C and (b) (W,Ti)C-5 vol.%CNT sintered from powders after milling for 10 h.

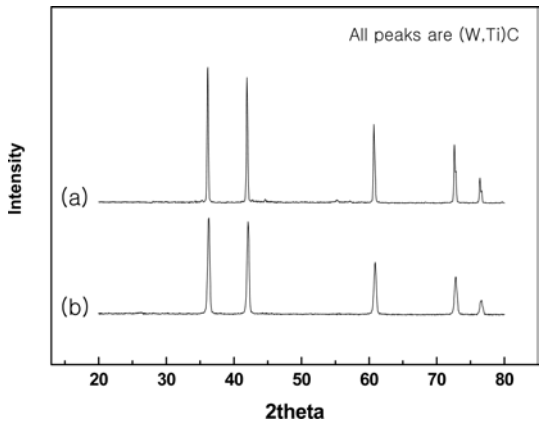

Fig. 6. XRD patterns of (a) (W,Ti)C and (b) (W,Ti)C-5 vol.%CNT sintered from powders after milling for 10 h.

Fig. 5 shows FE-SEM images of (W,Ti)C and (W,Ti)C-5 vol.%CNT sintered from the 10 h milled powders. From the figures, it is known that the (W,Ti)C is consisted of nanoparticle. And their corresponding relative density is about 99%. (Ti,W)C powder was synthesized by carbothermal reduction at 1200 ºC for 1 h from the rutile TiO_2 ,WO_3 and C powders. The use of conventional sintering at 1510 ºC to successfully consolidate (Ti,W)C powder was demonstrated by Kang et al. [11]. The synthesized nanopowder of (Ti,W)C with an average grain size of 40 nm was consolidated at 1510 ºC for 1h under a vacuum($\sim 10^{-4}$ atm) to a fully dense (Ti,W)C with an average grain size of 1~2 μm. The mechanical properties of homogeneous (Ti,W)C have Hv values in the range of 19-21 GPa and K_{IC} values of 6.4-7.7 MPa.$m^{1/2}$. Comparing the above study with ours, the sintering temperature and time of the high frequency induction heated sintering is lower and shorter than those of conventional sintering. The hardness (2822 kg/mm^2) of (Ti,W)C in our study is higher than that of Kang et al. [11] due to refinement of grain size.

Fig. 6 shows the XRD patterns of the (W,Ti)C and (W,Ti)C-5vol.%CNT sintered for milled powders used in this study. All peaks are from (W,Ti)C. Plots of B_r ($B_{crystalline} + B_{strain}$) cosθ versus sinθ in Suryanarayana

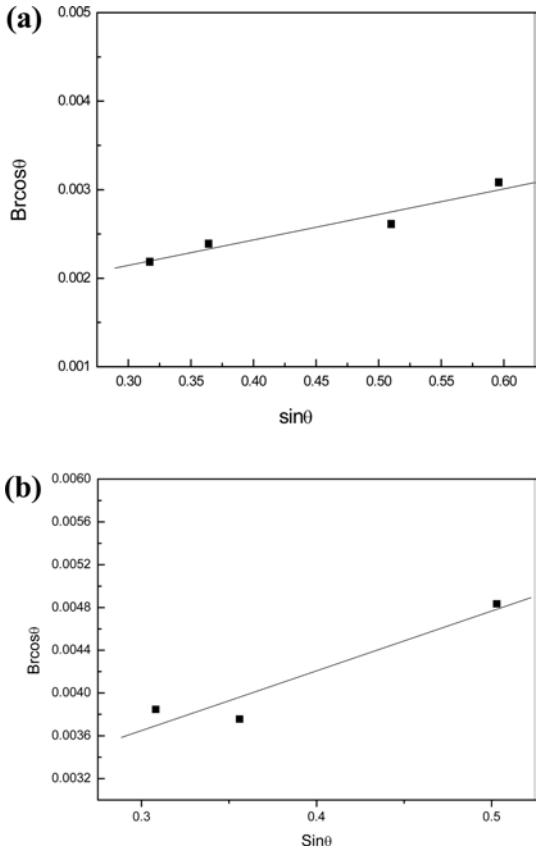

Fig. 7. Plots of B_r ($B_{crystallite} + B_{strain}$) cosθ versus sinθ for (W,Ti)C in (a) (W,Ti)C-0 vol%CNT and (b) (W,Ti)C-5 vol.%CNT sintered from powders after milling for 10 h.

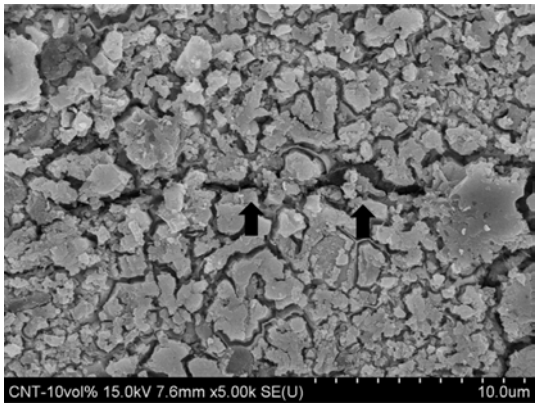

Fig. 8. Median crack propagating of the (W,Ti)C-5 vol.%CNT sintered from powder milled for 10 h.

and Grant Norton's formula [16] are shown in Fig. 7. The average grain sizes of the (W,Ti)C in 0vol.%CNT and 5 vol.%CNT calculated from the XRD data were about 62 and 70 nm. Thus, the average grain size of the sintered (W,Ti)C is not greatly larger than that of the initial powder, indicating the absence of much grain growth during sintering. This retention of the grain size is attributed to the high heating rate and the relatively short term exposure of the powders to the high temperature.

The role of the current (resistive or inductive) in sintering has been the focus of several attempts aimed at providing an explanation of the observed enhancement of sintering and the improved characteristics of the products. The role played by the current has been variously interpreted, the effect being explained in terms of a fast heating rate due to Joule heating, the presence of a plasma in pores separating powder particles, and the intrinsic contribution of the current to mass transport [17-20].

Vickers hardness measurements were performed on polished sections of the (W,Ti)C and (W,Ti)C-5vol.%CNT samples using a 10 kg_f load and 15 s dwell time. Indentations with large enough loads produced radial cracks emanating from the corners of the indent. The lengths of these cracks permit estimation of the fracture toughness of the materials by means of the expression [21]:

$$K_{IC} = 0.023(c / a)^{-3/2} \cdot H_v \cdot a^{1/2} \quad (2)$$

where c is the trace length of the crack measured from the center of the indentation, a is one half of the average length of the two indent diagonals, and H_v is the hardness. Hardness of (W,Ti)C and (W,Ti)C-5 vol.%CNT samples with ball milling for 10 h was 2822 and 1882 $kg{\cdot}mm^{-2}$, and their fracture toughness was 7, and 12 $MPa{\cdot}m^{1/2}$, respectively. These values represent the average of five measurements. A higher magnification view of the indentation median crack in a (W,Ti)C-5 vol.%CNT sample is shown in Fig. 8, which shows that the crack propagated in a deflective manner (↑). The addition of CNT to (W,Ti)C significantly improved the fracture toughness. The enhanced fracture toughness of (W,Ti)C-CNT composite is believed that CNT in the composite may deter the propagation of cracks

Summary

Nanopowder of (W,Ti)C was fabricated by high energy ball milling. Using the rapid sintering method, HFIHS, the densification of (W,Ti)C and (W,Ti)C-5vol.%CNT was accomplished using high energy ball milling. The average grain sizes of the (W,Ti)C in 0vol.%CNT, and 5 vol.%CNT calculated from the XRD data were about 62 and 70 nm and their corresponding densities were approximately 99%, respectively. The Vickers Hardness of (W,Ti)C, and (W,Ti)C-5 vol.%CNT samples with ball milling for 10 h was 2822, and 1882 $kg{\cdot}mm^{-2}$, and their fracture toughness was 7, and 12 $MPa{\cdot}m^{1/2}$, respectively. The enhanced fracture toughness of (W,Ti)C-CNT composite is believed that CNT in the composite may deter the propagation of cracks

Acknowledgments

This study was supported by a grant in aid awarded by the Basic Research Project of the Korea Institute of

Geoscience and Mineral Resources (KIGAM), funded by the Ministry of Science, ICT and Future Planning (GP2015036) and this work was supported by the Korea Institute of Energy Technology Evaluation and Planning(KETEP) and the Ministry of Trade, Industry & Energy(MOTIE) of the Republic of Korea (No. 20164030201070) and this research was supported by Basic Science Research Program though the National Research Foundation of Korea (NRF) funded by the Ministry of Education (2015R1D1A1A01056600).

References

1. S. Imasato, K. Tokumoto, T. Kitada, and S. Sakaguchi, Int. J. Refract. Met. Hard Mater. 13[5] (1995) 305-312.
2. E.A. Almond, and B. Roebuck, Mater. Sci. Eng. A 105/106 (1988) 237-248.
3. G. Gille, J. Bredthauer, B. Gries, and B. Mende, Int. J. Refract. Met. Hard Mater. 18[2-3] (2000) 87-102.
4. P. Goeuriot, F. Thevenot, N. Bouaoudja, and G. Fantozzi, Ceram. Int. 13[2] (1987) 99-103.
5. E.T. Thostenson. C. Li, and T. Chou, Compos. Sci. Technol. 65[3-4] (2005) 491-516.
6. M. Sherif El-Eskandarany, J. Alloys Compd. 305[1-2] (2000) 225-238.
7. In-Jin Shon, Hyoung-Gon Jo, Byung-Su Kim, Jin-Kook Yoon, and Kyung-Tae Hong, Korean J. Met. Mater., 53 (2015) 474-479.
8. I. J. Shon, H. G. Jo, and H. J. Kwon, Korean J. Met. Mater., 52 (2014) 343-346.
9. A.I.Y. Tok, L.H. Luo, and F.Y.C. Boey, Mater. Sci. Eng. A 383 (2004) 229-234.
10. H.G. Jo, and I.J. Shon, Journal of Ceramic Processing Research 15[6] (2014) 371-375.
11. J. Jung, and S. Kang, Scripta Mater. 56 (2007) 561-564.
12. I. J. Shon, Korean J. Met. Mater., vol. 52, no. 8 (2014) 573-584.
13. H. S. Kang, J. M. Doh, J. K. Yoon, and I. J. Shon, Korean J. Met. Mater., vol. 52, no. 10 (2014) 777-782.
14. So-Mang Kwon, Na-Ra Park, Jae-Won Shin, Se-Hoon Oh, Byung-Su Kim, and In-Jin Shon, Korean J. Met. Mater., 53 (2015) 555-562.
15. Bo-Ram Kang and In-Jin Shon, Korean J. Met. Mater., 53 (2015) 320-325.
16. C. Suryanarayana, and M. Grant Norton, X-ray Diffraction A Practical Approach, Plenum Press, New York, (1998).
17. Z. Shen, M. Johnsson, Z. Zhao, and M. Nygren, J. Am. Ceram. Soc. 85 (2002) 1921-1927.
18. J.E. Garay, U. Anselmi-Tamburini, Z.A. Munir, S.C. Glade and P. Asoka-Kumar, Appl. Phys. Lett. 85 (2004) 573-577.
19. J.R. Friedman, J.E. Garay, U. Anselmi-Tamburini and Z.A. Munir, Intermetallics 12[6] (2004) 589-596.
20. J.E. Garay, J.E. Garay. U. Anselmi-Tamburini and Z.A. Munir, Acta Mater. 51 (2003) 4487-4493.
21. K. Niihara, R. Morena, and D.P.H. Hasselman, J. Mater. Sci. Lett. 1 (1982) 12-16.